Molecular Gas, Dust and Star Formation in Galaxies
Proceedings IAU Symposium No. 292, 2012
T. Wong & J. Ott, eds.
© 2012 International Astronomical Union
DOI: 00.0000/X000000000000000X

Molecules as tracers of galaxy evolution

Susanne Aalto[1]

[1]Department of Earth and Space Sciences, Chalmers University of Technology
Onsala Space Observatory, SE-439 92 Onsala, Sweden
email: saalto@chalmers.se

Abstract. Studying the molecular phase of the interstellar medium in galaxies is fundamental for the understanding of the onset and evolution of star formation and the growth of supermassive black holes. We can use molecules as observational tools exploiting them as tracers of chemical, physical and dynamical conditions. In this short review, key molecules (e.g. HCN, HCO^+, HNC, HC_3N, CN, H_3O^+) in identifying the nature of buried activity and its evolution are discussed including some standard astrochemical scenarios. Furthermore, we can use IR excited molecular emission to probe the very inner regions of luminous infrared galaxies (LIRGs) allowing us to get past the optically thick dust barrier of the compact obscured nuclei, e.g. in the dusty LIRG NGC4418. High resolution studies are often necessary to separate effects of excitation and radiative transport from those of chemistry - one example is absorption and effects of stimulated emission in the ULIRG Arp220. Finally, molecular gas in large scale galactic outflows is briefly discussed.

Keywords. galaxies: evolution — galaxies: ISM — galaxies:active —- radio lines: ISM —- ISM: molecules — ISM:abundances —- astrochemistry

1. Introduction

Spectacular bursts of star formation and feeding of supermassive black holes (SMBHs) occur when collisions of gas-rich galaxies funnel massive amounts of molecular gas and dust into nuclei of luminous and ultra luminous infrared galaxies (LIRGs/ULIRGs). There are several reasons why molecular emission and absorption are very useful tools to study the nature and evolution of LIRGs and ULIRGs. Molecules are fundamentally important since they serve as fuel for the evolution of galaxies through star formation and the growth of SMBHs. The discovery of molecular gas in large scale galactic outflows also suggests that molecules play a part in the turning-off of starbursts and AGNs. Furthermore, mm and submm emission can penetrate highly obscured regions allowing us to probe the dusty nuclei of LIRGs and ULIRGs revealing the nature of the buried activity.

Here, the use of molecules as tracers of extragalactic astrochemistry is introduced in section 2. Useful molecular lines are presented in section 3 and in section 4 some global line ratios and examples of spectral scans are discussed. Effects of IR radiation on molecular excitation is presented in section 5. In section 6 the importance of studying molecular chemistry and excitation at high resolution is discussed including new interferometric results on molecular gas in large scale outflows and winds.

2. Extragalactic astrochemistry

The CO 1–0 line is often used to trace H_2 mass (e.g. Paglione et al. 2001; Wada & Tomisaka 2005; Narayanan et al. 2012) and gas dynamics. The line intensity ratio between CO and the polar molecule HCN is a popular measure of the mass fraction of dense ($n > 10^4$ cm^{-3}) molecular gas (e.g. Gao & Solomon 2004). Astrochemistry offers an additional new tool to study galaxy evolution - in particular in deeply dust-obscured objects. We can study both the radiative and

dynamical impact on the gas properties and its chemistry and hence develop scenarios for the evolution of molecular gas in galaxies. There are a number of standard scenarios often referred to when we discuss extragalactic astrochemistry:

(*a*) **Photon (or Photo) dominated region (PDR)** Regions are affected by far-ultraviolet photons (energy hν=6 - 13.6 eV). The surface temperatures may be large (300 - 1000 K) but bulk temperatures are expected to be moderate (20 - 50 K) due to the layered structure of the PDR. The chemistry is dominated by photo-chemistry (e.g. Hollenbach & Tielens 1997). The penetration of the UV photons is limited by dust and, as A_V increases, cosmic rays take over as the dominant source of ionization reactions. The heating occurs through photoelectric effect on grains and PAHs, collisional de-excitation of H_2.

(*b*) **X-ray dominated region (XDR)** These regions are affected by X-rays with hν=1-100 keV providing a larger penetration depth than in PDRs and a more efficient heating mechanism. Thus XDRs are signified by large bulk temperatures > 100 K and a chemical structure typical of the special ion-neutral chemistry triggered by the irradiation of X-rays. (e.g. Maloney et al. 1996; Lepp & Dalgarno 1996; Meijerink & Spaans 2005). The ionization occurs through primary X-rays and secondary photo electrons. The heating occurs through Coulomb heating, H_2 ionization, H_2 vibrational excitation, and dissociative excitation. The ionization rate is high (from the secondary photo electron).

(*c*) **Cosmic ray dominated region (CDR or CRDR)** – Regions of elevated ($> 10^3 \times$ Galactic value) cosmic ray energy density (e.g. Suchkov et al. 1993; Meijerink et al. 2011; Bayet et al. 2011) primarily originating from supernovae.

(*d*) **Dense shielded regions** In warm, dusty and dense regions, that are relatively shielded from harmful radiation, hot core-like chemistry may dominate with temperatures ranging from 50 to 500 K (e.g. Nomura & Millar 2004; Viti 2005). Icy grain mantles are released affecting chemistry and the intense infrared (IR) radiation fields impact the molecular excitation (Costagliola & Aalto 2010; Sakamoto et al. 2010). Formation and survival of complex species result in rich chemistry.

(*e*) **Mechanically dominated region** The chemistry reflects the speed of the shock and thus the level of grain processing (e.g. Usero et al. 2007; Viti et al. 2011; Kazandjian et al. 2012). Milder shocks results in the icy mantles coming off - and in more violent shocks the grain cores may be affected. Shock temperatures can be very high ranging from 100 K (C-shocks) up to a few thousand K (J-shocks). The dissipation of turbulence act on the bulk of the gas and may heat the gas to C-shock temperatures.

It is likely that within one resolving beam we have multiple scenarios represented. However, we have a large variety of spectral tools at our disposal allowing us to probe a wide range of physical environments, temperatures and densities of the interstellar medium. Combining molecular species and transitions with spatial resolution and sensitivity will enable us to disentangle chemical scenarios and to separate effects of excitation and radiative transfer from those of chemistry.

3. Some useful molecular emission lines and ratios

A summary of molecular species detected in extragalactic sources can be found in Martín et al. (2011). By 2011, a total of 46 species and 23 isotopic variants had been identified. With the advent of ALMA this list will grow significantly in the coming years. Intensity ratios of emission lines between species are often used to identify various astrochemical scenarios and/or physical conditions in the gas. Below is a list of a few popular molecular lines and ratios.

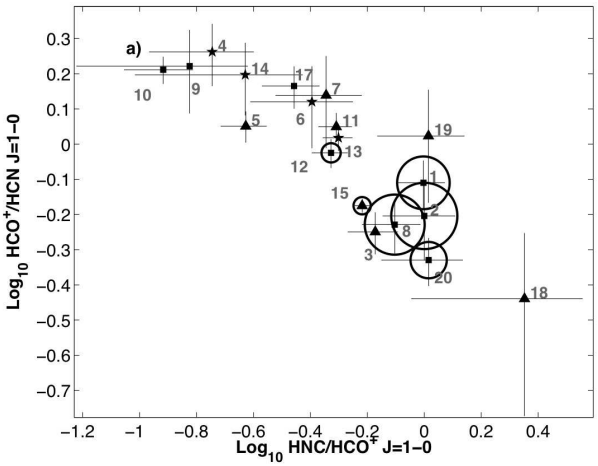

Figure 1. Plot of the HCO^+/HCN vs. the HNC/HCO^+ 1–0 line ratio for a sample of luminous LIRGs, ULIRGs and AGNs (Costagliola et al. 2011). The circles indicate galaxies with HC_3N 10–9 detections where the diameter of the circle is proportional to the HC_3N 10–9/HCN 1–0 line ratio. Error bars show 1σ uncertainties. The HC_3N luminous galaxies are also HNC-bright with respect to HCO^+ and HCN. The lines were observed simultaneously with the IRAM 30m EMIR receiver.

• **Molecular ions: HCO^+ and H_3O^+** In the molecular cores around some AGNs elevated HCN/HCO^+ 1–0 intensity ratios have been found (e.g. Kohno 2003; Imanishi et al. 2009) and also in some ULIRGs (Graciá-Carpio et al. 2006). A suggested interpretation is that this is a chemical effect due to the presence of an XDR. However, theoretical models are not in agreement on whether the HCO^+ abundance is suppressed or enhanced relative to HCN in XDRs (e.g. Maloney et al. 1996; Meijerink & Spaans 2005). Furthermore, HCN/HCO^+ 1–0 abundance ratios >1 are also expected in dense shielded gas (e.g. Aalto et al. 2007a) and in gas heated by shocks (e.g. Kazandjian et al. 2012). *Thus, it is possible that HCN/HCO^+ 1–0 ratios are generally enhanced in compact molecular regions towards galaxy nuclei - regardless off the nature of the buried activity*. For H_3O^+, models predict an order of magnitude greater abundances in XDRs than in PDRs. The first extragalactic 364 GHz detections seem to support this notion (van der Tak et al. 2008; Aalto et al. 2011). It is however possible that elevated H_3O^+/H_2O ratios are also consistent with CDRs - this requires further investigation.

• **Isomers: HNC** In cold (T < 24 K) gas HNC/HCN abundance ratios are expected to be greater than unity while in dense, warmer gas and in shocked gas X(HCN)>X(HNC) (Schilke et al. 1992). However, in XDRs and PDRs X(HCN)$\gtrsim X$(HNC) also in warm gas (Meijerink & Spaans 2005) which complicates the use of the HCN/HNC abundance ratio as a tracer of gas temperature. Surveys reveal that global HCN/HNC 1–0 intensity ratios in luminous galaxies often range between 1 and 6 (e.g. Aalto et al. 2002; Baan et al. 2010), but there are cases where the HNC/HCN 3–2 intensity ratio exceeds unity (Aalto et al. 2007b, 2009). The cause for this "overluminosity of HNC (e.g. in Arp 220 - see Fig. 3) has been suggested to be either due to excitation and/or to effects of IR-pumping of HNC (see section on excitation below). In some XDR models the HNC abundances may also exceed those of HCN by a factor of two, but for this effect to lead to I(HNC) > I(HCN) the optical depth of the lines has to be fairly low.

• **Shielded gas: HC_3N** Surveys have revealed a subset of luminous galaxies with unusually bright HC_3N 10–9 emission compared to HCN 1–0 (Lindberg et al. 2011; Costagliola et al. 2011). HC_3N is destroyed by UV and particle radiation and in the Galaxy it can be found in high abundance in hot cores and in general in dense, warm and shielded gas. Interestingly, surveys reveal bright HC_3N line emission from

LIRGs/ULIRGs with deep IR silicate absorption features and warm FIR colours suggesting a preference for dust obscured galaxies with high A_V and deeply buried (young?) activity.

• **Radicals: CN** In contrast to HC_3N, enhancement of CN is expected in XDRs and in PDRs (e.g. Aalto et al. 2002; Baan et al. 2010; Meijerink & Spaans 2005). CN is also chemically linked to HCN via photodissociation. The abundance enhancement of CN over HCN is greater in an XDR (factors 40 - 1000) than in a PDR (CN/HCN abundance ratio range from 0.5 to 2) (Lepp & Dalgarno 1996; Meijerink & Spaans 2005). Other radicals, such as CH, NO and OH are also more enhanced (relative to HCN) in an XDR than in a PDR and the CH/HCN column density for example may exceed 10^3.

• **Shock tracers: SiO, H_2O, HNCO, CH_3OH** Shocks can form SiO through the sputtering of Si from silicate grain cores, followed by reactions between the released Si and O_2 or OH (Guillet et al. 2009). The shock must therefore be strong enough to get the Si off the grains while species such as H_2O, HNCO, CH_3OH can be released in milder events resulting in the icy grain mantle coming off and releasing them into the gas phase.

• **Gas temperature: NH_3, H_2CO** The relative populations of the K_a ladders of the (slightly) asymmetric top molecule H_2CO are generally governed by collisions and inter-ladder line ratios are thus generally good tracers of the gas kinetic temperature. Mühle et al. (2007) observed para-H_2CO in the starburst M82 to deduce the presence of 200 K molecular gas. The inversion-rotation transitions of NH_3 may also be used to accurately determine gas kinetic temperature (e.g. Martin & Ho 1986).

• **Isotopomers** Isotopic variants (isotopomers) - e.g. ^{13}C, ^{18}O, ^{15}N of species can help measure optical depth variations and thus map out the structure of the interstellar medium and find changes in the physical conditions. For example, variations in the CO/ ^{13}CO 1–0 intensity ratio that map the dynamical effects on clouds in spiral arms and bars and/or effects of temperature gradients (e.g. Meier et al. 2000; Tosaki et al. 2002; Aalto et al. 1997, 2010; Hirota et al. 2010). Globally the CO/ ^{13}CO 1–0 intensity ratio increases rather strongly with dust temperature an effect that can largely be explained as a gas temperature effect (e.g. Aalto et al. 1995; Costagliola et al. 2011). Studying isotopic variants will also give important information on stellar nucleosynthesis and the number of stellar generations the ISM has gone through.

Note that these are emission lines in the mm and submm regime - a more complete list would for example include absorption line diagnostics and higher-frequency lines observed by e.g. the Herschel space observatory (van der Werf et al. 2010; González-Alfonso et al. 2010). For example, Meijerink et al. (2011) suggest observing a combination of species, OH^+, OH, H_2O^+, H_2O and H_3O^+, to distinguish between CDRs and XDRs - many of these species are best studied at THz frequencies with the Herschel telescope or with ALMA.

4. Global line ratios and spectral scans

There are a large number of studies using global molecular line ratios to attempt to classify galaxies in terms of nuclear activity and evolutionary status (e.g. Aalto et al. 1995; Paglione et al. 2001; Aalto et al. 2002; Gao & Solomon 2004; Graciá-Carpio et al. 2006; Krips et al. 2008; Baan et al. 2010; Papadopoulos et al. 2010) Although effects of radiative transfer and excitation are difficult to account for in these surveys, they are useful in identifying trends and searching for correlations. These relations may then be further explored with multi-transition observations as well as higher resolution studies.

The new broadband receivers - mounted on interferometers such as the SMA, PdBI and ALMA, and on single dish telescopes including the IRAM 30m telescope - allow several lines to be measured simultaneously improving the accuracy of the line ratios. One such example is

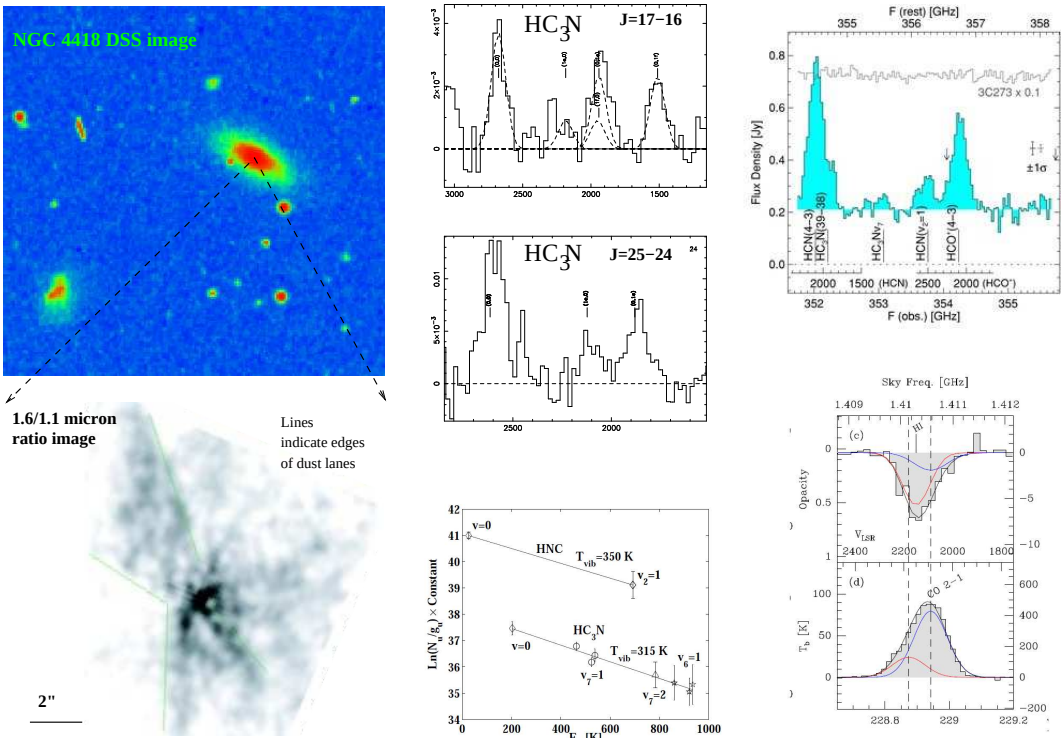

Figure 2. Upper left: DSS image of the LIRG NGC4418. Lower left: NICMOS NIR image of the ratio of the 1.6/1.1 μm continuum revealing the dusty interior of NGC4418 (Evans et al. 2003). Upper center: Two spectra of intense HC_3N emission - rotational and vibrational - from NGC4418 and below the spectra is a rotational diagram of HC3N and HNC. Upper right: SMA spectrum with HCN 4–3 and v_2=1, HCO^+ 4–3, HC_3N 39-38 and v_7=1 (Sakamoto et al. 2010). Lower right: Merlin HI absorption (top) and SMA CO 2–1 emission showing evidence for infalling gas towards the nucleus of NGC4418 (Costagliola et al., 2012, submitted)

.

the EVOLUTION study on the IRAM 30m where the 3mm EMIR backend was used to observe spectral properties of 25 infrared luminous galaxies selected from the IR PAH (polycyclic aromatic hydrocarbons)-silicate diagnostic diagram of Spoon et al. (2007). Simultaneous observations of HCN, HCO^+, HNC, HC_3N, C_2H, SiO and CO, ^{13}CO, $C^{18}O$, CN were carried out to look for correlations Costagliola et al. (2011). The HCO^+/HCN 1–0 ratio is correlated with the PAH equivalent width suggesting that there is a connection to PDRs. However, In general it was found that HNC and HCO^+ 1–0 emission appear anti correlated (see Fig. 1) - which is difficult to explain with standard PDR models and it is suggested that mechanical heating must be added to the models (e.g. Baan et al. 2010; Costagliola et al. 2011; Meijerink et al. 2011). All HNC-bright objects are either luminous IR galaxies (LIRG) or Seyferts. Galaxies with bright PAH emission show low HNC/HCO^+ ratios. Note, however, that variations in the ratios between HCN, HNC and HCO^+ are relatively small. Stronger effects are obtained for fainter species such as HC_3N . The only HC_3N detections are in objects with HCO^+ /HCN 1–0 intensity ratios < 1 (see Fig. 1). Galaxies with the highest HC_3N/HCN ratios have warm IRAS colours (60/100 μm > 0.8) and it is suggested that *HC_3N is a tracer of young, dust enshrouded activity*.

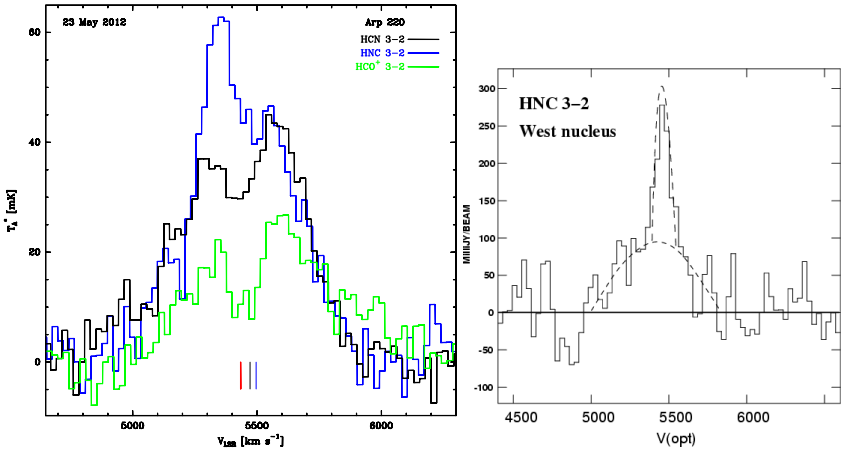

Figure 3. Left: Single dish (global profile) EMIR 1mm spectra of Arp220 showing I(HNC)>I(HCN)>I(HCO$^+$) 3–2 (S. Aalto et al. in prep.). Right: SMA HNC 3–2 spectrum of the western nucleus of Arp220 revealing a bright narrow feature suggested to be due to weak amplification of HNC (Aalto et al. 2009). (The emission feature coincides with a deep absorption feature in the HCO$^+$ 3–2 spectrum (Sakamoto et al. 2009).) Note the difference in velocity scales: the SMA HNC spectrum is in optical velocity which is approximately 100 km s^{-1} larger than the velocities for the radio definition in the left figure.

4.1. *Spectral scans*

Combining many lines simultaneously in a spectral scan will give a more complete (and complex) picture of the chemical status of a galaxy. This includes emission from rarer species with clearer diagnostic value. Spectral scans of the nearby starburst galaxies NGC253 and M82, and the starburst/Seyfert NGC1068 have been carried out at 1, 2 and 3 mm wavelength by the IRAM 30m and the Nobeyama 45m telescopes (e.g. Martín et al. 2006; Nakajima et al. 2011; Aladro et al. 2011, 2012). The chemistry of NGC 253 shows a similarity to that of the Galactic Center molecular clouds, which are thought to be dominated by low-velocity shocks. In contrast, the surveys of M82 reveal a PDR chemistry different from that of NGC253. For NGC1068 some of the carbon-chemistry appears similar to that of M82 while other aspects of the chemistry seem to be dominated by cosmic rays and XDRs. The ULIRG Arp220 has been surveyed in the 1mm band by the SMA interferometer (Martín et al. 2011) and the chemical composition seems consistent with an ISM heated by a young starburst and chemically enriched by consecutive bursts of star formation. Vibrationally excited emission from HC_3N and CH_3CN are indicative of a warm, intense IR field. With ALMA there is an ongoing spectral scan (bands 3, 6, 7, PI:Costagliola) of the LIRG NGC4418 where the spectrum is dominated by many rotational-vibrational lines of HC_3N (Aalto et al. 2007a; Costagliola & Aalto 2010; Sakamoto et al. 2010).

5. Molecular excitation - IR pumping of molecules

When we interpret mm and submm molecular spectra from external galaxies we usually assume that the excitation is dominated by collisions with H_2. However, there are also other possible mechanisms including IR radiative excitation where molecules absorb IR continuum corresponding to their bending modes. It is possible that this IR-pumping may affect the excitation of the rotational levels in the vibrational ground state. Thus, to correctly interpret the molecular emission we must examine its excitation. For example, both HCN and HNC can absorb IR-photons to the bending mode (its first vibrational state) and then it decays back to the ground state via its P-branch (v = 1-0, ΔJ = +1) or R-branch (v = 1-0, ΔJ = -1). In this way, a vibrational

excitation may produce a change in the rotational state in the ground level and can be treated (effectively) as a collisional excitation in the statistical equations. Thus, IR pumping excites the molecule to the higher rotational level by a selection rule $\Delta J = 2$. For HNC, the bending mode occurs at $\lambda = 21.5$ μm (464.2 cm^{-1}) with an energy level $h\nu/k = 669$ K and an A-coefficient of $A_{\rm IR} = 5.2$ s^{-1}. For HCN the mode occurs at $\lambda = 14$ μm (713.5 cm^{-1}), energy level $h\nu/k = 1027$ K and $A_{\rm IR} = 1.7$ s^{-1}. The pumping of HNC and HCN may start to become effective when the IR background reaches an optically thick brightness temperature of $T_{\rm B} \approx 50$ K and 85 K respectively - and for gas densities below critical.

Furthermore, recent results toward dust obscured galaxies show the presence of rotational lines from vibrationally excited HCN, HC_3N and (tentatively) HNC (Aalto et al. 2007a; Costagliola & Aalto 2010; Sakamoto et al. 2010; Martín et al. 2011). *These lines can be used to probe inside the optically thick dust cocoons in the nuclei of deeply obscured galaxies. One example of this is NGC4418 where the vibrational temperatures $T_{\rm vib}$ of HCN, HNC and HC_3N are 200-400 K suggesting the presence of a "hot core - heated either by an extremely compact young starburst or an embedded AGN. The size of this core has been determined to be $r < 5$ pc.*

6. Molecules at high spatial resolution

Interferometric studies provide both spatial resolution and sufficient pointing accuracy to allow us to separate regions of different dominant chemical processes. High resolution studies on IC 342 and Maffei 2 (Meier & Turner 2005, 2012) show that the HCN, HNC, HCO^+ 1-0 line emission and 3 mm continuum are tightly spatially correlated, indicating a close connection to star formation. In contrast, HNCO, and CH_3OH follow the molecular bar arms, especially the bar ends. This is probably caused by the spiral and bar shocks resulting in the icy grain mantles coming off. The C_2H emission prefers the starburst region (but is somewhat more extended) in Maffei 2 where it also is tracing a nuclear outflow. In IC342, C_2H is instead found near the nuclear star cluster (more evolved star formation) and not the current star formation.

There have been many studies of the chemistry of the nearby Seyfert galaxy NGC1068. High resolution interferometric observations of SiO and CN (García-Burillo et al. 2010) reveal that SiO is detected in a 400 pc circum nuclear disk (CND) around the AGN with SiO abundances (10^{-9}) more than one order of magnitude above those measured in the starburst ring. The overall abundance of CN in the CND is also high, 10^{-7}. Abundances measured for CN and SiO and the correlation of CN/COand SiO/COratios with hard X-ray irradiation suggest that the CND of NGC1068 has become a giant XDR.

6.1. *Molecular excitation - the compact nuclei of Arp220*

To correctly interpret molecular line ratios it is important to separate effects of excitation from those of chemistry. In some cases this can only be done at high spatial resolution. In the ULIRG Arp220 the HCN/HCO^+ 1–0 ratio is >1 at 1.″6 resolution (Imanishi et al. 2007) - this is suggested to be caused either by XDR chemistry and/or by IR pumping of HCN. However, a study at even higher resolution 0.″4 and at higher frequency (J=3–2 transition) of HCO^+ in Arp220 reveal an interesting effect: a big part of the HCO^+ spectrum is missing towards the eastern and western nuclei due to deep absorption toward the continuum (Sakamoto et al. 2009). The spectra are reminiscent of P-Cygni profiles and are indicative of outflowing gas from the two ULIRG nuclei. The absorption affects the global profile of HCO^+ 3–2 and it must be taken into account when drawing any conclusions on what is causing elevated HCN/HCO^+ intensity ratios in Arp220.

Interestingly, the HNC 3–2 profile towards the western nucleus has a prominent, narrow emission feature where HCO^+ shows absorption. This may constitute the *first ever detection of an HNC maser* - even if the amplification is weak (Aalto et al. 2009). This maser emission may be

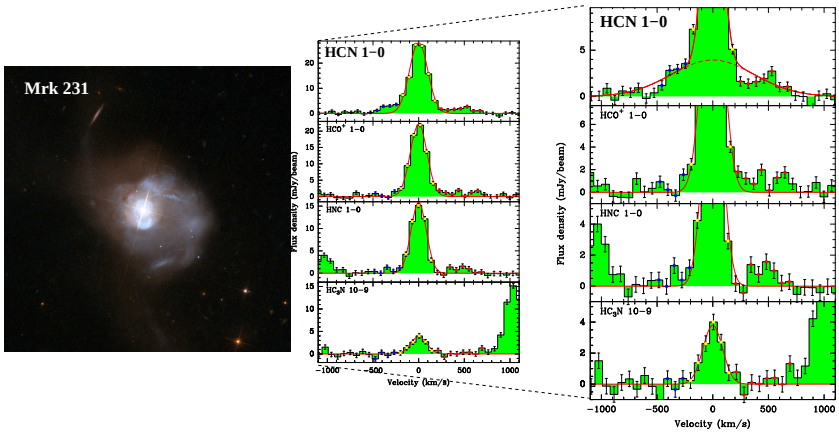

Figure 4. Left: HST image of Mrk231. Center and Right: Plateau de Bure interferometric spectra of HCN HCO^+ HNC 1–0 and HC_3N 10–9. In the right panels we have zoomed in on the base of the line to show the line wings more clearly. Red solid lines show Gaussian fits to the line center line widths. In the top right panel two Gaussians are fitted (Aalto et al. 2012a).

pumped by the 21.5 μm continuum emission. Recently a possible methanimine (H_2CNH) maser (Rickert et al. 2011) has been detected towards the same source.

6.2. *Molecular outflows*

Outflows driven by AGNsand/or starbursts represent a strong and direct mechanism for feedback that may clear central regions or the whole galaxy of fuel for future star formation or black hole (BH) growth. Many galactic winds and outflows carry large amounts of molecular gas and dust with them. There is a growing list of examples of molecular gas in outflows including: Early type galaxies: NGC1266 (Alatalo et al. 2011), NGC1377 (Aalto et al. 2012b); Interacting starburst LIRGs: NGC3256 (Sakamoto et al. 2006; Sakamoto 2012), M82 (Nakai et al. 1987; Walter et al. 2002), NGC2146 (Greve et al. 2000; Tsai et al. 2009); NGC253 (e.g. García-Burillo et al. 2000); NGC 1614 (Garcia-Burillo *et al.* 2012, in prep.); ULIRGs and AGNs: Mrk231 (e.g. Fischer et al. 2010; Feruglio et al. 2010; Aalto et al. 2012a; Cicone et al. 2012); M51 (Matsushita et al. 2007); LIRG and ULIRG surveys: (e.g. Baan 2007; Chung et al. 2011; Sturm et al. 2011); and high redshift QSOs: SWIRE survey (e.g. Polletta et al. 2011; Nesvadba et al. 2011).

Studying the physical and chemical conditions of the outflowing molecular gas will help us understand the driving mechanism, origin of the gas and its fate in the wind. Detection of bright SiO emission in a supershell and chimney of M82 (García-Burillo et al. 2001) show shock processed dust grain chemistry in the starburst wind. Imaging of low-*J* CO lines in the extreme, high-velocity wind of the QSO ULIRG Mrk231 (e.g. Feruglio et al. 2010; Cicone et al. 2012) can be used to study the excitation of the lower density gas in the outflow. *Interestingly, the Mrk 231 outflow has very bright HCN 1–0 emission* (Aalto et al. 2012a) (see Fig. 4) and emission from HNC and HCO^+ 1–0 is also detected in the outflow. Very recent PdBI imaging shows that the broad line wings are also present in the HCN 3–2 and 2–1 spectra (Aalto *et al.* in prep.). The HCN 1–0 flux actually rivals that of CO 1–0 in the outflow - so, why is HCN so bright? There are several options: a) Large numbers of dense clumps in the outflow. b) Extremely large HCN abundances and c) mid-IR pumping of HCN. If the outflow is extended beyond the reach of an optically thick mid-IR source of at least 85 K then c) can be ruled out. The low CO excitation (Cicone et al. 2012) indicates that only some of the volume can be filled with dense clumps which leaves a combination of a) and b). High HCN abundances are expected in warm regions, e.g. in AGNs (e.g. Harada et al. 2010) or in shocks (e.g. Tafalla et al. 2010; Kazandjian et al.

2012) and a possibility is that elevated HCN luminosity is a signature of AGN-driven outflows. However, with a current sample of only one, this requires more study.

References

Aalto, S., Beswick, R., & Jütte, E. 2010, A&A, 522, A59
Aalto, S., Booth, R. S., Black, J. H., & Johansson, L. E. B. 1995, A&A, 300, 369
Aalto, S., Costagliola, F., van der Tak, F., & Meijerink, R. 2011, A&A, 527, A69
Aalto, S., Garcia-Burillo, S., Muller, S., et al. 2012a, A&A, 537, A44
Aalto, S., Monje, R., & Martín, S. 2007a, A&A, 475, 479
Aalto, S., Muller, S., Sakamoto, K., et al. 2012b, A&A, 546, A68
Aalto, S., Polatidis, A. G., Hüttemeister, S., & Curran, S. J. 2002, A&A, 381, 783
Aalto, S., Radford, S. J. E., Scoville, N. Z., & Sargent, A. I. 1997, ApJ, 475, L107
Aalto, S., Spaans, M., Wiedner, M. C., & Hüttemeister, S. 2007b, A&A, 464, 193
Aalto, S., Wilner, D., Spaans, M., et al. 2009, A&A, 493, 481
Aladro, R., Martín, S., Martín-Pintado, J., et al. 2011, A&A, 535, A84
Aladro, R., Viti, S., Bayet, E., et al. 2012, ArXiv e-prints
Alatalo, K., Blitz, L., Young, L. M., et al. 2011, ApJ, 735, 88
Baan, W. A. 2007, New A Rev., 51, 149
Baan, W. A., Loenen, A. F., & Spaans, M. 2010, A&A, 516, A40
Bayet, E., Williams, D. A., Hartquist, T. W., & Viti, S. 2011, MNRAS, 414, 1583
Chung, A., Yun, M. S., Naraynan, G., Heyer, M., & Erickson, N. R. 2011, ApJ, 732, L15+
Cicone, C., Feruglio, C., Maiolino, R., et al. 2012, A&A, 543, A99
Costagliola, F. & Aalto, S. 2010, A&A, 515, A71
Costagliola, F., Aalto, S., Rodriguez, M. I., et al. 2011, A&A, 528, A30
Evans, A. S., Becklin, E. E., Scoville, N. Z., et al. 2003, AJ, 125, 2341
Feruglio, C., Maiolino, R., Piconcelli, E., et al. 2010, A&A, 518, L155+
Fischer, J., Sturm, E., González-Alfonso, E., et al. 2010, A&A, 518, L41
Gao, Y. & Solomon, P. M. 2004, ApJS, 152, 63
García-Burillo, S., Martín-Pintado, J., Fuente, A., & Neri, R. 2000, A&A, 355, 499
García-Burillo, S., Martín-Pintado, J., Fuente, A., & Neri, R. 2001, ApJ, 563, L27
García-Burillo, S., Usero, A., Fuente, A., et al. 2010, A&A, 519, A2
González-Alfonso, E., Fischer, J., Isaak, K., et al. 2010, A&A, 518, L43
Graciá-Carpio, J., García-Burillo, S., Planesas, P., & Colina, L. 2006, ApJ, 640, L135
Greve, A., Neininger, N., Tarchi, A., & Sievers, A. 2000, A&A, 364, 409
Guillet, V., Jones, A. P., & Pineau Des Forêts, G. 2009, A&A, 497, 145
Harada, N., Herbst, E., & Wakelam, V. 2010, ApJ, 721, 1570
Hirota, A., Kuno, N., Sato, N., et al. 2010, PASJ, 62, 1261
Hollenbach, D. J. & Tielens, A. G. G. M. 1997, ARA&A, 35, 179
Imanishi, M., Nakanishi, K., Tamura, Y., Oi, N., & Kohno, K. 2007, AJ, 134, 2366
Imanishi, M., Nakanishi, K., Tamura, Y., & Peng, C. 2009, AJ, 137, 3581
Kazandjian, M. V., Meijerink, R., Pelupessy, I., Israel, F. P., & Spaans, M. 2012, A&A, 542, A65
Kohno, K. 2003, in Astronomical Society of the Pacific Conference Series, Vol. 289, The Proceedings of the IAU 8th Asian-Pacific Regional Meeting, Volume 1, ed. S. Ikeuchi, J. Hearnshaw, & T. Hanawa, 349–352
Krips, M., Neri, R., García-Burillo, S., et al. 2008, ApJ, 677, 262
Lepp, S. & Dalgarno, A. 1996, A&A, 306, L21
Lindberg, J. E., Aalto, S., Costagliola, F., et al. 2011, A&A, 527, A150
Maloney, P. R., Hollenbach, D. J., & Tielens, A. G. G. M. 1996, ApJ, 466, 561
Martin, R. N. & Ho, P. T. P. 1986, ApJ, 308, L7
Martín, S., Krips, M., Martín-Pintado, J., et al. 2011, A&A, 527, A36
Martín, S., Mauersberger, R., Martín-Pintado, J., Henkel, C., & García-Burillo, S. 2006, ApJS, 164, 450
Matsushita, S., Muller, S., & Lim, J. 2007, A&A, 468, L49
Meier, D. S. & Turner, J. L. 2005, ApJ, 618, 259

Meier, D. S. & Turner, J. L. 2012, ApJ, 755, 104
Meier, D. S., Turner, J. L., & Hurt, R. L. 2000, ApJ, 531, 200
Meijerink, R. & Spaans, M. 2005, A&A, 436, 397
Meijerink, R., Spaans, M., Loenen, A. F., & van der Werf, P. P. 2011, A&A, 525, A119
Mühle, S., Seaquist, E. R., & Henkel, C. 2007, ApJ, 671, 1579
Nakai, N., Hayashi, M., Handa, T., et al. 1987, PASJ, 39, 685
Nakajima, T., Takano, S., Kohno, K., & Inoue, H. 2011, ApJ, 728, L38
Narayanan, D., Krumholz, M. R., Ostriker, E. C., & Hernquist, L. 2012, MNRAS, 2537
Nesvadba, N. P. H., Polletta, M., Lehnert, M. D., et al. 2011, MNRAS, 415, 2359
Nomura, H. & Millar, T. J. 2004, A&A, 414, 409
Paglione, T. A. D., Wall, W. F., Young, J. S., et al. 2001, ApJS, 135, 183
Papadopoulos, P. P., van der Werf, P., Isaak, K., & Xilouris, E. M. 2010, ApJ, 715, 775
Polletta, M., Nesvadba, N. P. H., Neri, R., et al. 2011, A&A, 533, A20
Rickert, M., Momjian, E., Sarma, A., & AO Arp 220 Team. 2011, in Bulletin of the American Astronomical Society, Vol. 43, American Astronomical Society Meeting Abstracts #217, #332.01
Sakamoto, K. 2012, ArXiv e-prints
Sakamoto, K., Aalto, S., Evans, A. S., Wiedner, M. C., & Wilner, D. J. 2010, ApJ, 725, L228
Sakamoto, K., Aalto, S., Wilner, D. J., et al. 2009, ApJ, 700, L104
Sakamoto, K., Ho, P. T. P., & Peck, A. B. 2006, ApJ, 644, 862
Schilke, P., Walmsley, C. M., Pineau Des Forets, G., et al. 1992, A&A, 256, 595
Spoon, H. W. W., Marshall, J. A., Houck, J. R., et al. 2007, ApJ, 654, L49
Sturm, E., González-Alfonso, E., Veilleux, S., et al. 2011, ApJ, 733, L16+
Suchkov, A., Allen, R. J., & Heckman, T. M. 1993, ApJ, 413, 542
Tafalla, M., Santiago-García, J., Hacar, A., & Bachiller, R. 2010, A&A, 522, A91
Tosaki, T., Hasegawa, T., Shioya, Y., Kuno, N., & Matsushita, S. 2002, PASJ, 54, 209
Tsai, A.-L., Matsushita, S., Nakanishi, K., et al. 2009, PASJ, 61, 237
Usero, A., García-Burillo, S., Martín-Pintado, J., Fuente, A., & Neri, R. 2007, New A Rev., 51, 75
van der Tak, F. F. S., Aalto, S., & Meijerink, R. 2008, A&A, 477, L5
van der Werf, P. P., Isaak, K. G., Meijerink, R., et al. 2010, A&A, 518, L42
Viti, S. 2005, in IAU Symposium, Vol. 231, Astrochemistry: Recent Successes and Current Challenges, ed. D. C. Lis, G. A. Blake, & E. Herbst, 67–76
Viti, S., Jimenez-Serra, I., Yates, J. A., et al. 2011, ApJ, 740, L3
Wada, K. & Tomisaka, K. 2005, ApJ, 619, 93
Walter, F., Weiss, A., & Scoville, N. 2002, ApJ, 580, L21